Supporting Information (SI)

Kinetic Adsorption Profile and Conformation Evolution at the DNA-Gold Nanoparticle Interface Probed by Dynamic Light Scattering

Wenjie Wang,[†] XiaoFan Ding,[†] Miao He,[‖] Jing Wang,[†] Xinhui Lou[†]*

(†) Department of Chemistry, Capital Normal University, Xisanhuan North Road. 105, Beijing 100048,China; (‖) School of Environment, Tsinghua University, Beijing 100084, China.

The synthesis of gold nanoparticles, the kinetic DLS measurements during the DNA/AuNP complex preparation course, the quantification of the DNA capacity on AuNPs by UV-vis and fluorescent measurements, and derivation of the Lagergren-first-order rate and pseudo second-order rate model as the function of D_h increase over incubation time, Figure S1-9, and Table S-1were provided here in order.

Experimental Section

Synthesis of 13 nm AuNPs. All glassware was cleaned in aqua regia (HCl: HNO_3 =3: 1), rinsed with millipore water and then dried in oven prior to synthesis. AuNPs were synthesized based on the standard citrate reduction process. Briefly, an aqueous solution of $HAuCl_4$ (1 mM, 200 mL) was heated and refluxed for 10 min while stirring. And then the trisodium citrate solution (38.8 mM, 20 mL) was quickly added which resulted in an immediately solution color change from pale to yellow to wine red. After 15 min refluxing, the solution was slowly cooled to room temperature and subsequently filtered through a 0.22 μm cellulose nitrate filter. The final gold nanoparticle solution was ~10 nM through the measurement of UV-Vis adsorption spectroscopy. The solution was stored at 4 ^{o}C.

Kinetic Study of the Preparation Process of PolyAs/AuNPs and Aptamers/AuNPs via DLS Measurements. To generate free thiol groups for surface immobilization, 40 μL stock thiolated polyAs and aptamers (Table S-1) at 100 μM was mixed with 40 μL DTT (0.1 M) and 1.6 μL TEA at room temperature for 30 min. The freshly reduced DNA sequences were subsequently purified through the desalting NAP-5 columns pre-equilibrated with phosphate buffer (PB, 10 mM, pH 7.4) and quantified by UV-Vis absorption at 260 nm. The purified DNA probes in PB (1000 μL) were then mixed with AuNPs (initial concentration of 10 nM) at the molar ratio at 500:1. The DNA preparation process of DNA/AuNPs included three steps: 1) the 17 hr-aging step, where no NaCl was added into the sample, 2) the salt adding step, where the concentration of NaCl in the sample gradually increased from 0 to 0.3 M by stepwisely adding PB buffer (pH 7.4) containing 1 M NaCl from the 17 to 28 hr, and 3) the incubation step from the 28 to 40 hr with no more salt added. The sizes of the DNA /AuNP conjugates were in-situ continuously monitored by the DLS measurements at the selected time points. During the salt adding step, after each measurement, the sample was adjusted to the desired NaCl concentration by three additions of the equal volume of PB buffer containing 1 M NaCl every 30 min, followed by the DLS measurement in 30 min. The volume of PB buffer required was calculated according to the desired NaCl concentration.

Quantification of the DNA Capacity on AuNPs by UV-Vis Measurements. During or after the preparation process, the excessive DNAs were removed by centrifugation at 13000 rpm for 30 min. The concentration of DNAs in the supernatant was determined by the adsorption at 260 nm. The total amount of DNAs on AuNPs were then calculated by subtracting the amount of DNAs in the supernatant from the initial input DNAs. The capacity of DNAs per particle was finally calculated by dividing the total amount of DNAs on AuNPs by the amount of AuNPs.

Quantification of the DNA Capacity on AuNPs by Fluorescent Measurements. The FAM-modified thiolated polyA$_{30}$ was reduced as described above and mixed with AuNPs at the molar ratio at 500:1. During the aging step, FAM-polyA$_{30}$ /AuNP conjugates aliquots were taken at each time point of 0.2, 0.5, 1, 2, 6, 10, 17 hr during the aging step and purified by centrifugation at 13000 rpm for 30 min. To determine the capacity of FAM-polyA$_{30}$ on AuNPs, the purified FAM-polyA$_{30}$ /AuNP conjugates were displaced by overnight incubation in 1 M DTT in 0.2 M PB, pH 7.4. The Au precipitate was then removed by centrifugation and the fluorescence intensity of the supernatant was subsequently measured. The excitation wavelength was 493 nm and the emission was collected at 522 nm. All measurements were repeated three times to obtain error bars.

Derivation of the Lagergren-first-order rate and pseudo second-order rate model as the function of D_h increase over incubation time. There are two typical kinetic models in the study of adsorption kinetics on liquid-solid interface, the Lagergren-first-order rate and pseudo second-order rate model.[1] In an adsorption process, it is supposed that the rate (dq_t/dt) is proportional either to the difference between the amount of adsorption at time t and at equilibrium (q_e-q_t) or to the square of the difference, respectively, for these two models. Let k_f be the proportionality constant, we have

$$\frac{dq_t}{dt} = k_f(q_{e1} - q_t) \qquad (1)$$

Where q_{e1} and q_t are the amount of substance adsorbed (g/kg) on solid surface at equilibrium or at time t (hr) per gram of adsorbent, respectively, and K_f is the equilibrium rate constant of Lagergren-first-order (hr^{-1}). After integration, we get $\log(q_{e1} - q_t) = \log q_{e1} - \frac{K_f}{2.303} t$ (2)

Eq. (2) is called the Lagergren-first-order equation.

Or, let k_s be the proportionality constant, we have

$$\frac{dq_t}{dt} = k_s (q_{e2} - q_t)^2 \quad (3)$$

Where q_{e2} and q_t are the amount of substance adsorbed (g/Kg) on solid surface at equilibrium or at time t (hr) per gram of adsorbent, and K_s is the equilibrium rate constant of the pseudo-second-order rate constant (hr^{-1}). After integration, we get

$$\frac{t}{q_t} = \frac{1}{K_s q_{e2}^{\ 2}} + \frac{1}{q_{e2}} t \quad (4)$$

Eq. (4) is called the pseudo second-order model.

In the DILOT conformation model, the D_h increase is proportional to the sorption capacity (or the amount of substance adsorbed). Thus, the derivation of the equation (2) and (4) was shown below:

$$q_{e1} = kd_{e1},\ q_{e2} = kd_{e2},\ q_t = kd_t \quad (5-7)$$

Where d_{e1} and d_t are the D_h increases (nm) caused by adsorption of DNAs on AuNP at equilibrium or at time t (hr), and k is the proportionality constant between the hydrodynamic size increases and the amount of DNAs adsorbed on AuNPs.

Then, the equations (5-7) were substituted into the equation (2) to get the equation (8):

$$\log k + \log(d_{e1} - d_t) = \log k + \log d_{e1} - \frac{K_f}{2.303} t$$

$$\log(d_{e1} - d_t) = \log d_{e1} - \frac{K_f}{2.303} t \quad (8)$$

Where K_f is the equilibrium rate constant of Lagergren-first-order.

And the equations (5-7) were substituted into the equation (4) to get the equation (9):

$$\frac{t}{kd_t} = \frac{1}{K_s k^2 d_{e2}^2} + \frac{1}{kd_{e2}} t$$

$$\frac{t}{d_t} = \frac{1}{K_s k d_{e2}^2} + \frac{1}{d_{e2}} t$$

$$\frac{t}{d_t} = \frac{1}{K_S^{'} d_{e2}^2} + \frac{1}{d_{e2}} t \qquad (9)$$

K_s' = $K_s \bullet k$, is the equilibrium rate constant of the pseudo-second-order rate constant.

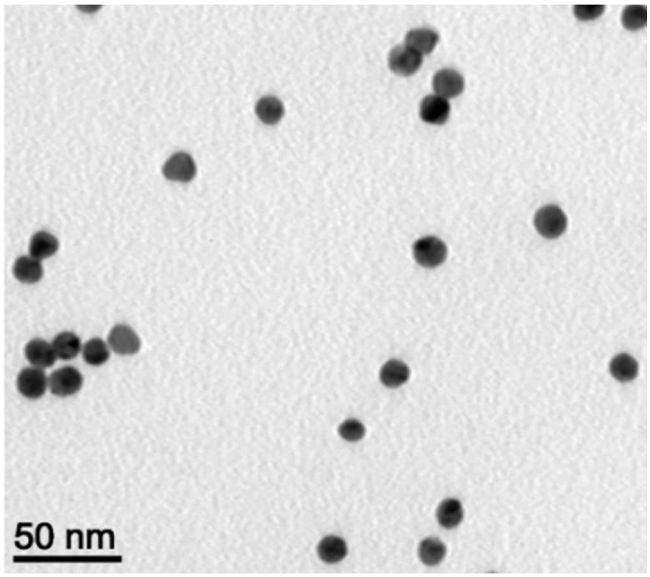

Figure S-1. Transmission electron microscope images of the AuNPs prepared in this study. The measured diameter is 13 ± 0.4 nm.

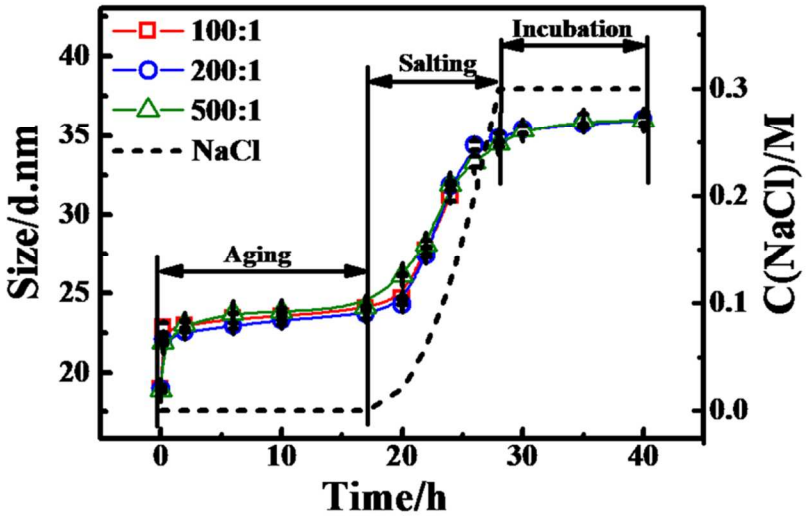

Figure S-2. Kinetic measurements of the D_h values of polyA$_{44}$/AuNP during the typical aging-salting preparation procedure at the different molar ratios of polyA$_{44}$ to AuNPs: 500: 1, 200:1, and 100:1, respectively. The procedure includes the aging step (without adding NaCl, from 0 to 17 hr), the salting step (stepwisely adding 1 M NaCl phosphate buffer to gradually increase the concentration of NaCl up to 0.3 M, from 17 to 28 hr), and incubation step (without further increase of NaCl concentration, from 28 to 40 hr). The dotted line represents the NaCl concentration of the sample in the procedure. The errors were calculated from the three repeated measurements. At the molar ratios of 100:1, there were two distribution peaks when the concentration of NaCl was higher than 0.2 M due to the bad stability of the complex. Therefore no data points were shown at the concentration of NaCl higher than 0.2 M. The determined loading of polyA$_{44}$ on AuNP at the end of the immobilization procedure was only 42±1 strands per particle, which was significantly lower than those obtained at the high molar ratio of 200:1 and 500:1 (76 ±3 and 74±7 strands per particle, respectively). Therefore, in this study, the high molar ratio of 500:1 was used to ensure the good stability of the complex during the process and to achieve the high surface coverage of AuNPs.

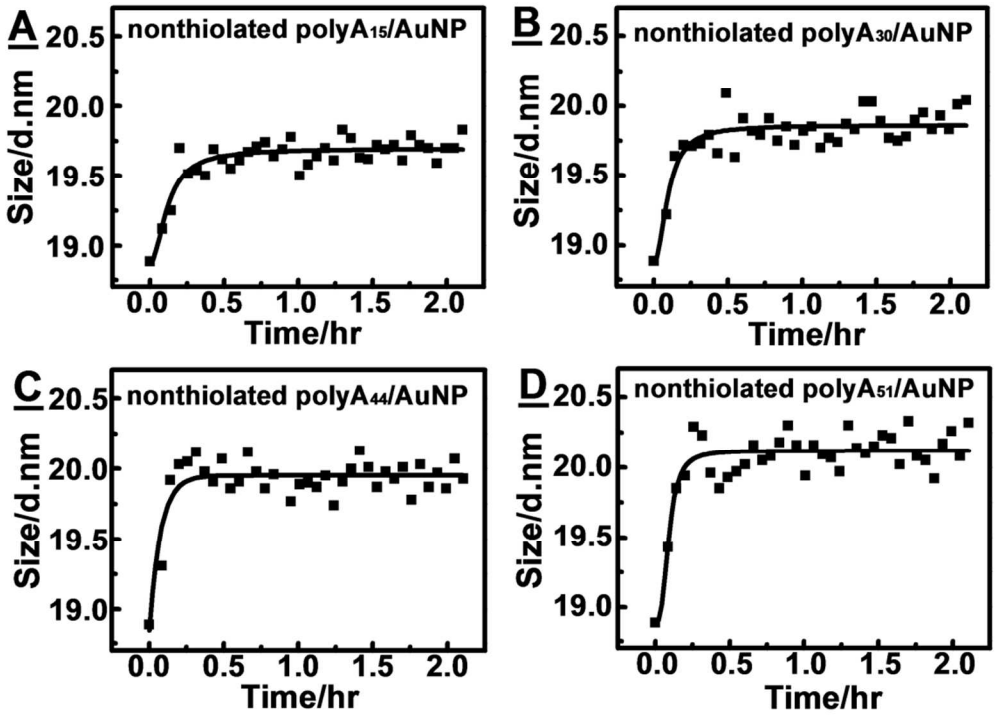

Figure S-3. Kinetic measurements of the D_h values of AuNPs during the immobilization process of the nonthiolated polyAs with different lengths onto the 13 nm AuNPs in phosphate buffer (10 mM, pH 7.4) by DLS measurements. The molar ratios of the polyAs to AuNPs were all 500: 1.

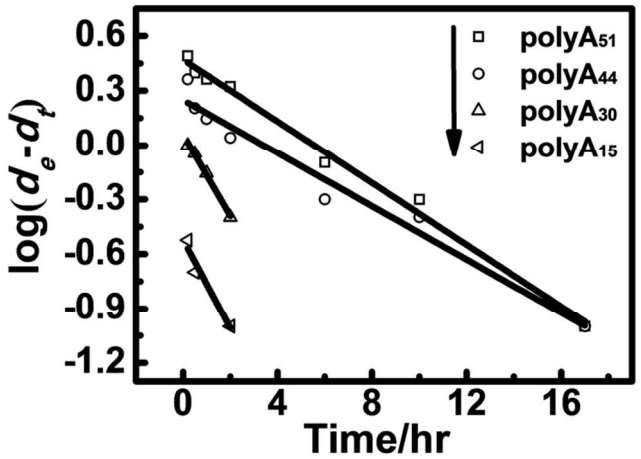

Figure S-4. Lagergren-first-order adsorption kinetics of thiolated polyAs onto AuNPs in the aging step.

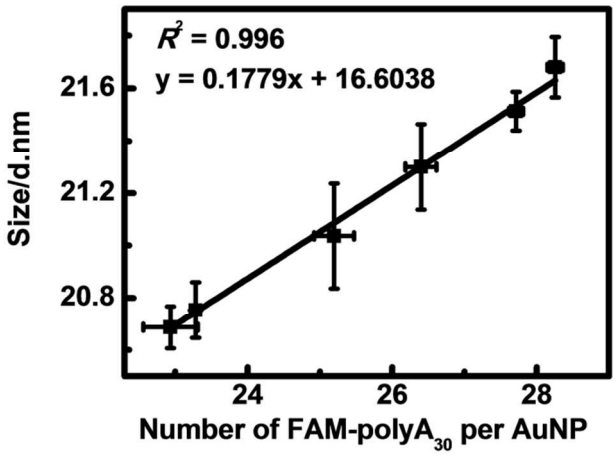

Figure S-5. The linear relationship between the D_h values of FAM-polyA30/AuNP in the aging step and the surface capacity. The errors were calculated from the three repeated experiments.

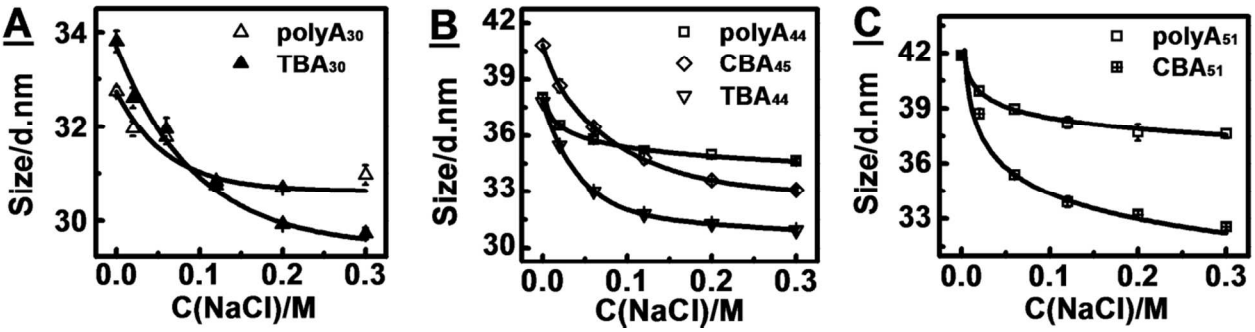

Figure S-6. Direct comparisons of the salt effects on the D_h values of the polyA /AuNP and aptamer /AuNP conjugates prepared according to the procedures shown in the caption of Figure 1 by DLS measurements. The errors were calculated from the three repeated measurements.

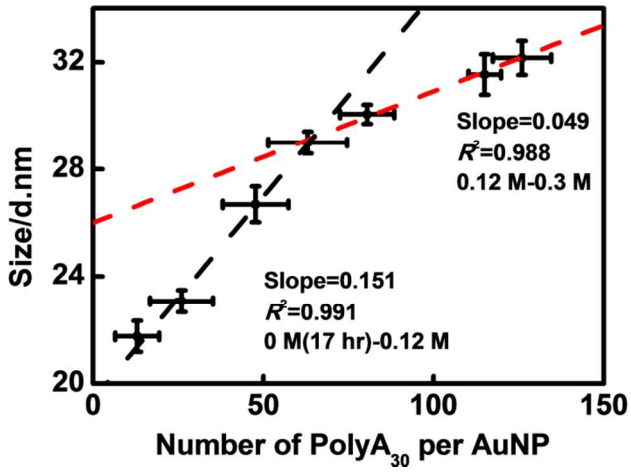

Figure S-7. The relationship between the D_h values of polyA$_{30}$ /AuNP conjugates prepared in the salting and incubation step and the surface capacity. The conjugates were all centrifuged and resuspended in 10 mM PB prior to the DLS measurements. The errors were calculated from the six repeated experiments.

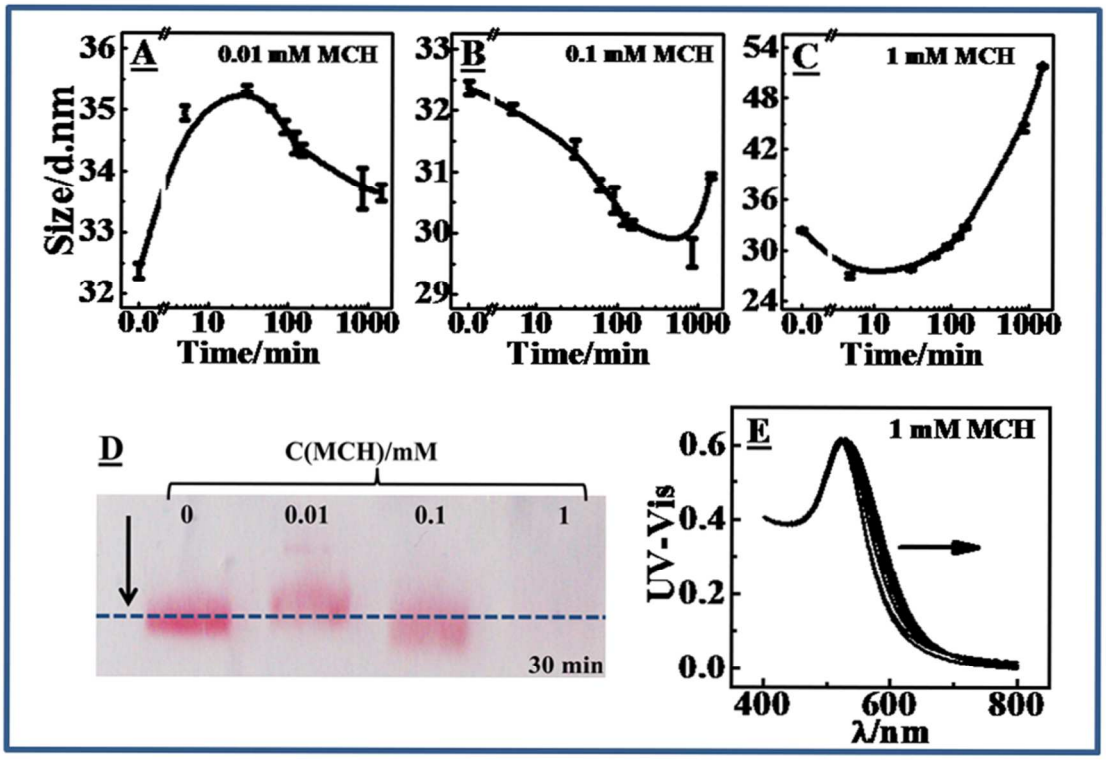

Figure S-8. The effects of MCH treatment on the D_h values (A, B, and C), the mobility (B), and the UV-vis adsorption (E) of polyA$_{30}$/AuNP. The three bands on the 2% agarose gel are the polyA$_{30}$/AuNP before (left) and after (middle and right) 30 min incubation with 0.01 and 0.1 mM MCH, respectively. No band was observed for the conjugate after 30 min's incubation with 1 mM MCH.

Discussion:

Theoretically, there are four types of interactions between MCH and the surface of AuNPAs. The first type interaction involves the occupying of the open area that is not bound with the bases and the thiol group of DNAs, resulting in no significant size change. The second type interaction is to replace the bases of DNAs that is adsorbed on the surface of AuNPs since the thiol group can bind with Au with much stronger affinity compared to the bases of the DNAs. This replacement of the bases should cause the significant increase of the size. The third type interaction is the displacement of the thiol group of DNA that is adsorbed on the surface of AuNP. This displacement would cause the release of the DNA from the surface of AuNPs and the size decrease. The forth type interaction is the interaction of two thiol groups

with two AuNPs, resulting in the cross linking and aggregation of the AuNPs. These steps may happen simultaneously; however, the dominant interactions may be different under varied conditions.

Our data clearly reflects the conformational change of DNA on AuNP after MCH treatment under different conditions and agrees with the surface chemistry very well (Figure S-8). Specifically, when DNA/AuNP was incubated with 0.01 mM MCH (Figure S-8A), we observed the increase of the size in the first 30 min's incubation and a decrease of the size after that (Figure S-8A). The data suggests that the second type interaction is dominant in the first 30 min's incubation and the inner layer indeed exists even at the end of the incubation step. The increase of the size was further confirmed by the smaller mobility of the conjugate on the gel electrophoresis (Figure S-8D, 0.01 mM MCH). The decrease of the size after the longer time incubation with MCH implies that the third type interaction is dominant.

The domination of the third type interaction becomes prominent when DNA/AuNP was incubated with the higher concentration of MCH (0.1 mM). The increase of the size due to the second type interaction wasn’t able to be observed any more. We observed the continuous decrease of the size from the beginning of the incubation with MCH (Figure S-8B) until 500 min’s incubation. The decrease of the size was further confirmed by the greater mobility of the conjugate on the gel electrophoresis (Figure S-8D, 0.1 mM MCH).

Further increase of the concentration of MCH to 1 mM, we observed the decrease of the size in the first 30 min and the continuous and big increase of the size after that (Figure S-8C). The big size increase was due to the partially aggregation of AuNPs caused by the forth type of interaction. The aggregation was confirmed by the red-shift of the plasmon band in the UV-vis measurements (Figure S-8E). The partially aggregation also caused the bad stability of the conjugate and no band was observed on the gel electrophoresis (Figure S-8D, 1 mM MCH).

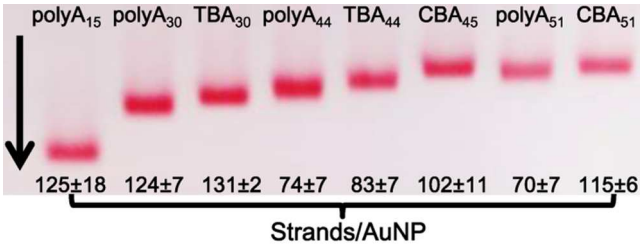

Figure S-9. 2% agarose gel of the AuNPs that fully coated with the thiolated polyAs ($polyA_{15}$, $polyA_{30}$, $polyA_{44}$, and $polyA_{51}$) and aptamers (TBA_{30}, TBA_{44}, and CBA_{45}, CBA_{51}) in the order as indicated in the photo. All the conjugates were concentrated in PB buffer before loading. The numbers of DNAs per AuNP calculated via UV-vis measurements were listed under each lane.

Table S-1. Thiolated oligonucleotides used in this study

name	sequence (from 5′ to 3′)
$polyA_{15}$	HS-$(CH_2)_6$-A_{15}
$polyA_{30}$	HS-$(CH_2)_6$-A_{30}
$polyA_{44}$	HS-$(CH_2)_6$-A_{44}
$polyA_{51}$	HS-$(CH_2)_6$-A_{51}
TBA_{30}	HS-$(CH_2)_6$-A_{15}GGTTGGTGTGGTTGG
TBA_{44}	HS-$(CH_2)_6$-A_{15}AGTCCGTGGTAGGGCAGGTTGGGGTGACT
CBA_{45}	HS-$(CH_2)_6$-A_{15}GACAAGGAAAATCCTTCAATGAAGTGGGTC
CBA_{51}	HS-$(CH_2)_6$-A_{15}GGAGACAAGGAAAATCCTTCAATGAAGTGG GTCGAC

(1) Fu, H.-Z.; Wang, M.-H.; Ho, Y.-S. *J. Colloid Interface Sci.* **2012,** *379*, 148-156.